Journal of Power Sources 262 (2014) 372–379

Contents lists available at ScienceDirect

Journal of Power Sources

journal homepage: www.elsevier.com/locate/jpowsour

Enhanced proton conductivity of proton exchange membranes by incorporating sulfonated metal-organic frameworks

Zhen Li [a,b], Guangwei He [a,b], Yuning Zhao [a,b], Ying Cao [a,b], Hong Wu [a,b,c], Yifan Li [a,b], Zhongyi Jiang [a,b,*]

[a] Key Laboratory for Green Chemical Technology, Ministry of Education of China, School of Chemical Engineering and Technology, Tianjin University, Tianjin 300072, China
[b] Collaborative Innovation Center of Chemical Science and Engineering (Tianjin), Tianjin 300072, China
[c] Tianjin Key Laboratory of Membrane Science and Desalination Technology, Tianjin University, Tianjin 300072, China

HIGHLIGHTS

- Sulfonated MOFs were filled into proton exchange membrane for the first time.
- Multi-functional sulfonated MOFs enhanced the proton conduction in membrane.
- The hybrid membrane showed high proton conductivity up to 0.306 S cm^{-1}.

ARTICLE INFO

Article history:
Received 13 November 2013
Received in revised form
27 February 2014
Accepted 25 March 2014
Available online 15 April 2014

Keywords:
Sulfonated metal-organic framework
MIL101
Sulfonated poly(ether ether ketone)
Proton exchange membrane
Proton conductivity

ABSTRACT

In this study, octahedral crystal MIL101(Cr) with a uniform size of ~400 nm is synthesized via hydrothermal reaction. It is then functionalized with sulfonic acid groups by concentrated sulfuric acid and trifluoromethanesulfonic anhydride in nitromethane. The sulfonated MIL101(Cr) are homogeneously incorporated into sulfonated poly(ether ether ketone) (SPEEK) matrix to prepare hybrid membranes. The performances of hybrid membranes are evaluated by proton conductivity, methanol permeability, water uptake and swelling property, and thermal stability. The methanol permeability increased slightly from 6.12×10^{-7} to 7.39×10^{-7} cm^2 s^{-1} with the filler contents increasing from 0 to 10 wt. %. However, the proton conductivity of the hybrid membranes increased significantly. The proton conductivity is increased up to 0.306 S cm^{-1} at 75 °C and 100% RH, which is 96.2% higher than that of pristine membranes (0.156 S cm^{-1}). The increment of proton conductivity is attributed to the following multiple functionalities of the sulfonated MIL101(Cr) in hybrid membranes: i) providing sulfonic acid groups as facile proton hopping sites; ii) forming additional proton-transport pathways at the interfaces of polymer and MOFs; iii) constructing hydrogen-bonded networks for proton conduction via −OH provided by the hydrolysis of coordinatively unsaturated metal sites.

1. Introduction

In recent years, metal-organic frameworks (MOFs) have drawn enormous attention in the fields of gas storage [1–3], selective separation [4,5], heterogeneous catalysis [6,7] and so forth due to their unique features such as designable framework architectures and tunable pore surfaces. Because of their potential in proton-conduction promotion, as well as good mechanical and thermal stabilities, MOFs have been investigated as promising proton-conducting candidates [8]. MOFs can construct efficient proton pathways via forming hydrogen-bonded networks in pores by judicious selection of organic ligands and metal centers [9–12]. Moreover, there are abundant sites in MOFs to be modified with functional groups for proton conduction, which endows MOFs with much potential for proton-conduction improvement [13–17]. For example, a highly proton-conductive MOF constructed by introducing water molecules into anionic layer frameworks as conducting media exhibited proton conductivity of 8×10^{-3} S cm^{-1} at ambient temperature, which was comparable to Nafion [18].

* Corresponding author. Key Laboratory for Green Chemical Technology, Ministry of Education of China, School of Chemical Engineering and Technology, Tianjin University, Tianjin 300072, China. Tel./fax: +86 22 23500086.
E-mail address: zhyjiang@tju.edu.cn (Z. Jiang).

http://dx.doi.org/10.1016/j.jpowsour.2014.03.123
0378-7753/

More recently, there have been two reports on MOFs as fillers for proton exchange membranes (PEMs), and the MOFs were confirmed effective in intensifying the proton conduction of the hybrid membranes. Incorporation of a two-dimensional MOF containing protonated tertiary amines as proton carriers into PVP enhanced the proton conductivity from 1.4×10^{-8} to 3.2×10^{-4} S cm^{-1} at 53% RH and 333 K [19]. A primary amine functionalized MOF (Fe-MIL-101-NH_2) was reacted with PPO-SO_3Cl to prepare hybrid membranes. Proton conductivity of hybrid membranes was increased to 0.25 S cm^{-1} at 90 °C and 100% RH. The enhancement of proton conductivity was caused by two factors: i) the abundant −OH provided by the hydrolysis of Fe(III) in MOFs could construct hydrogen-bonded networks for proton conduction; ii) sulfonimide on the MOFs/polymer interface formed additional pathway for proton conduction [20].

However, amine groups can reduce ion exchange capacity of the membranes, which limit the further enhancement of proton-conduction property. Sulfonic acid group is the most commonly employed functional group in the field of PEMs and possesses superior proton conductive capacity compared with amine group [21–23]. For example, proton conductivity of a family of isostructural MIL53(Al)-R (where R = −NH_2, −OH and −COOH, respectively) is 2.3×10^{-9}, 4.2×10^{-7} and 2.0×10^{-6} S cm^{-1}, respectively. The significant variation in proton conductivity is mainly attributed to the change in pKa of the functional groups (where the pKa = 4.74, 4.08 and 3.62 for −NH_2, −OH and −COOH, respectively) [22]. Hence, sulfonic acid group with a far lower pKa of −1 could lead to higher proton conduction [24]. It can be conjectured that if sulfonic acid functionalized MOFs are synthesized and incorporated into polymer to prepare hybrid membranes, the proton conductivity will be further increased.

In this study, sulfonated MIL101(Cr) was prepared and incorporated into sulfonated poly(ether ether ketone) (SPEEK) to fabricate hybrid membranes for direct methanol fuel cells. The successful synthesis and modification of MIL101(Cr) were confirmed by Fourier transform infrared spectroscopy (FT-IR), X-ray diffraction (XRD), field emission scanning electron microscopy (FESEM) and thermal gravimetric analysis (TGA). The effects of incorporating sulfonated MIL-101(Cr) on membrane performance, including proton conductivity, methanol permeability, water uptake, area swelling, morphology, and thermal stability, were investigated by alternating-current impedance (AC impedance), FESEM, TGA, differential scanning calorimetry (DSC) and so on.

2. Experiment

2.1. Materials and chemicals

Terephthalic acid (H_2BDC, analytical reagent (AR)) was purchased from J&K Scientific Ltd. Chromium(III) nitrate nonahydrate (AR) was supplied by Strem Chemicals Inc. Concentrated sulfuric acid (98 wt.%, AR) and hydrofluoric acid (HF, 40 wt.%, AR) were bought from Tianjin Jiangtian Chemical Scientific Ltd. Trifluoromethanesulfonic anhydride (Tf_2O, AR) and nitromethane (AR) were purchased from Aladdin-reagent. Dimethylformamide (DMF, AR) was purchased from Tianjin Guanfu Chemical Scientific Ltd. Poly(ether ether ketone) (PEEK) was supplied by Victrex England. All of the aforementioned reagents were used as received, without further purification. All the other materials and chemicals were commercially available with analytical pure degree, and used as received. Deionized water was used throughout this study.

2.2. Preparation of the modified MIL101(Cr)

2.2.1. Preparation and purification of MIL-101(Cr)

MIL-101(Cr) was synthesized via hydrothermal reaction as reported in literature [25]. H_2BDC (1.660 g), chromium(III) nitrate (4.000 g), deionized water (48.00 mL) and HF (0.4125 mL) were transferred into a hydrothermal reactor, and the mixture was kept at 220 °C for 8 h, and then cooled to room temperature along with furnace. The product was separated by centrifugation and washed with DMF until the supernatant fluid was colorless. After drying under vacuum at 40 °C till constant weight, a green powder was obtained, which was designated as raw-MIL101(Cr).

To remove excess H_2BDC and chromium(III) nitrate in the pores of MOFs, raw-MIL101(Cr) was stirred in DMF at 80 °C for 12 h twice and in EtOH at 78 °C for 12 h twice, and then dried under vacuum at 45 °C till constant weight. The obtained crystal was designated as pure-MIL101(Cr).

2.2.2. Sulfonation of pure-MIL101(Cr)

To sulfonate pure-MIL101(Cr), Tf_2O and concentrated sulfuric acid were used to react with the pure-MIL101(Cr) [26]. Tf_2O (2.170 mL) was added dropwise into the homogeneously-dispersed mixture of pure-MIL101(Cr) (1.5 g), concentrated sulfuric acid (0.754 mL) and nitromethane (80 mL). After stirring at 30 °C for 1 h, the final product was separated from the mixture by centrifugation and washed by water until the pH of supernatant fluid was natural pH, and then dried under vacuum. The final product was designated as sul-MIL101(Cr).

2.3. Sulfonation of PEEK

SPEEK was prepared via post-sulfonation [27]. Dried PEEK (28 g) was added into concentrated sulfuric acid (200 mL) at room temperature under vigorous stirring. After dissolution, the dark red solution was kept stirring at 50 °C for 9.5 h. The crude product obtained by decanting the dark red solution into excessive cold water under continuous agitation was washed with water until the pH of filtrate was neutral pH, and then dried at 60 °C under vaccum till constant weight. Sulfonation degree (DS) of SPEEK was determined by titration.

2.4. Preparation of membranes

The membranes were prepared by solution-casting method. SPEEK (0.65 g) was dissolved into DMF (6.5 mL) under stirring. A certain amount of pure-MIL101(Cr) or sul-MIL101(Cr) was well dispersed in above solution and stirred vigorously at 25 °C for 24 h. Membranes were formed by casting the mixture onto glass plates and dried at 60 °C for 12 h and at 80 °C for another 12 h. In order to activate the membranes, the membranes were immersed into 1.0 mol L^{-1} H_2SO_4 solution (20 mL) for 48 h and rinsed with water until the pH of filtrate reached natural pH, and then dried at 60 °C under vacuum. The hybrid membranes were designated as SPEEK/pure-MIL-X or SPEEK/sul-MIL-X, representing pure-MIL101(Cr) or sul-MIL101(Cr) as the filler, where X referred to the weight percentage of pure-MIL101(Cr) or sul-MIL101(Cr) relative to SPEEK matrix. SPEEK pristine membrane was prepared by the same procedure for comparison purpose.

2.5. Characterizations

The crystal structure of raw-MIL-101(Cr), pure-MIL-101(Cr) and sul-MIL-101(Cr) was confirmed by high-resolution powder XRD operated on a Rigaku D/max2500v/Pc (Cu Ka) instrument in a angular range of 1–12°, with a 0.02° step size and 4 s per step. IR

study on the sulfonated structure was carried out to confirm the successful functionalization of pure-MIL101(Cr). Samples (5 mg) mixed with KBr (750 mg) and pressed into self-supported pellets were tested on a Nicolet 6700 instrument (resolution 4 cm^{-1}, 4000–400 cm^{-1}). Sulphur content in sul-MIL101(Cr) was measured by XPS. Microstructure of membranes was observed using FESEM (Nanosem 430, operated at 10 keV) after being freeze-fractured in liquid nitrogen and then sputtered with gold. Morphology of MOFs was observed in the same way without being freeze-fractured in liquid nitrogen. TGA (NETZSCH-TG209 F3) of membranes was recorded from 40 °C to 800 °C at a heating rate of 10 °C min^{-1} under nitrogen atmosphere, TGA of MOFs was recorded in the same condition except in air atmosphere. In order to determine the glass transition temperature (T_gs) of the membranes, DSC measurement was carried out on a DSC 204 F1 NETZSCH instrument with a cooling or heating rate of 10 °C min^{-1} in nitrogen atmosphere. Samples were preheated from room temperature to 130 °C, and then cooled to 90 °C and reheated to 260 °C.

2.6. Water uptake and membrane swelling

Rectangular-shaped membranes were dried at 60 °C till constant weight (W_{dry}, g) and the area (A_{dry}, cm^2) of membranes were measured. Then, the membranes were soaked in water until fully hydrated. Following by wiping the water in the surfaces of membranes, the weights (W_{wet}, g) and areas (A_{wet}, cm^2) of membranes were measured. The water uptake and area swelling were the average of three measurements with an error within 5.0% and calculated based on the following equations (Eqs. (1) and (2)), respectively.

$$\text{Water uptake}\ (\%) = \frac{W_{wet} - W_{dry}}{W_{dry}} \times 100 \quad (1)$$

$$\text{Area swelling}\ (\%) = \frac{A_{wet} - A_{dry}}{A_{dry}} \times 100 \quad (2)$$

2.7. Methanol permeability

Methanol permeability (P, $cm^2\ s^{-1}$, tested in 2 mol L^{-1} methanol solution) was measured using a glass diffusion cell separated into two compartments. One compartment of cell was filled with methanol, the other compartment was filled with deionized water. The liquid in two compartments was under stirring. Membranes were sandwiched between two compartments. Methanol concentration in the water compartment was measured at set intervals using a gas chromatography (Agilent 6820) equipped with a thermal conductivity detector (TCD) and a DB624 column. Since the diffusion coefficient of water and methanol in SPEEK membrane was low enough, the flux of water and methanol could be neglected during the test. The methanol permeability could be calculated from Eq. (3). The final value of methanol permeability (P, $cm^2\ s^{-1}$) was the average of three measurements with an error within 5.0%:

$$P = \frac{SV_B l}{AC_{A0}} \quad (3)$$

where S is the slope of the straight line of concentration versus time, V_B is the volume of the solution in the water compartment, l is the membrane thickness, A is effective membrane area calculated by the inner diameter of the diffusion cell, and C_{A0} is the feed concentration of methanol (aq), respectively.

2.8. Proton conductivity

Proton conductivity (σ, S cm^{-1}) was estimated in a conductivity cell by the AC impedance spectroscopy method in horizontal direction using an electrochemical workstation (Princeton Parstat 2273 Electrochemical System).

Membrane samples were hydrated in water for 48 h prior to measurement. The membrane samples were then sandwiched into a platinum-plated two-point-probe cell and heated by water vapor to a series of certain temperature ranging from 30 to 75 °C. The data was recorded over a frequency range of 10–10^6 Hz with oscillating voltage of 20 mV. The proton conductivity (σ, S cm^{-1}) was calculated according to the following Eq. (4).

$$\sigma = \frac{l}{AR} \quad (4)$$

Where l and A are the distance between the two electrodes and the cross-sectional area of the membrane, respectively, and R is the membrane resistance derived from the low intersection of the high frequency semicircle on a complex impedance plane with Re (Hz) axis. Three repeated measurements are conducted and the standard deviations are below 5.0%.

3. Results and discussion

3.1. Characterization of the MOFs

The morphology of raw-MIL101(Cr), pure-MIL101(Cr) and sul-MIL101(Cr) observed by FESEM was shown in Fig. 1. Crystals with a uniform size of about 400 nm and octahedral configuration was observed. Comparing the three images, it could be found that the morphology of octahedral crystals would not be altered by the DMF and CH_2Cl_2 treatment, but was slightly altered by the sulfonation afterwards.

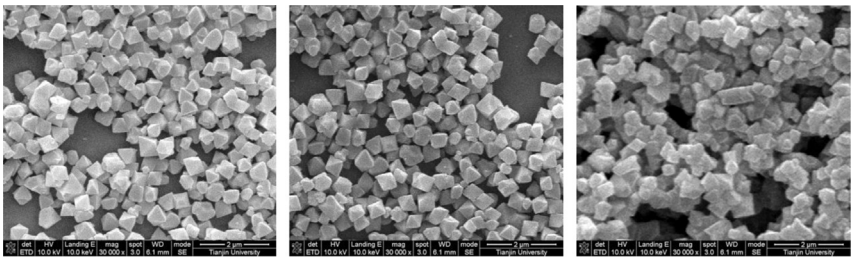

(a) (b) (c)

Fig. 1. FESEM images of (a) raw-MIL101(Cr), (b) pure-MIL101(Cr) and (c) sul-MIL101(Cr).

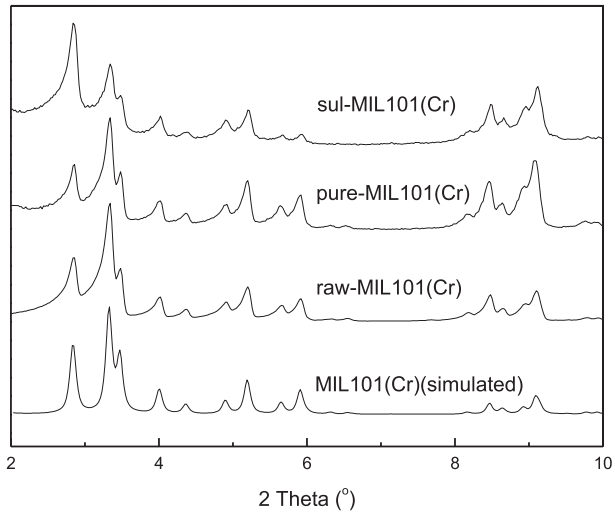

Fig. 2. Powder XRD patterns of simulation, raw-MIL101(Cr), pure-MIL101(Cr) and sul-MIL101(Cr).

XRD patterns of three kinds of MOFs were shown in Fig. 2 together with the simulated XRD pattern for MIL-101(Cr) [28], and the peak position of raw-MIL101(Cr) was consistent with the simulated pattern, which confirmed the formation of a pure phase of MIL101. The peaks position of pure-MIL101(Cr) and sul-MIL101(Cr) was the same as raw-MIL101(Cr), indicating that the crystal structure of MIL101 was unaffected after both purified by DMF and CH_2Cl_2 or sulfonated by concentrated sulfuric acid and Tf_2O.

The successful sulfonation was confirmed by FTIR and XPS as shown in Fig. 3 and Fig. 4, respectively. Compared with raw-MIL101(Cr), the spectrum of sul-MIL101(Cr) exhibited new peaks at 1255 and 1159 cm^{-1}, corresponding to the symmetric and asymmetric −S═O stretching vibrations, respectively. Moreover, the peak at 1110 cm^{-1} was responsible for the benzene rings substituted with a sulfonic acid group [26]. XPS was performed to determine the content of sulphur element (S) and the oxidation state of S. As shown in Fig 4, the peak of binding energy at around 167 eV indicated the hexavalent-oxidation state of S and the presence of S–O bond [29,30]. All these results demonstrated the successful sulfonation of pure-MIL-101. The content of sulphur

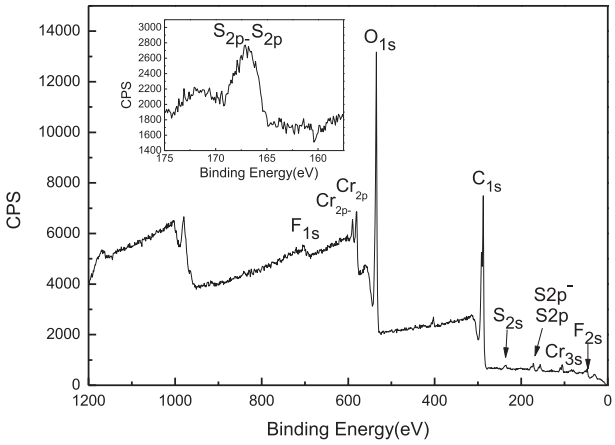

Fig. 4. XPS binding energy peak of sul-MIL101(Cr).

element could be calculated by the peak area ratio. The mass ratio of S was 2.03 wt.% and the atom ratio was 0.93 At%, indicating that 13.53% of terephthalic acid was sulfonated.

TGA was performed to determine the thermal stability of pure-MIL101(Cr) and sul-MIL101(Cr) as shown in Fig. 5. Three weight-loss steps were observed. Loss between 40 °C and 150 °C could be related to loss of water. Due to the decomposition of the framework, sharp weight loss was presented in the second step from 332 °C to 350 °C for pure-MIL101(Cr) and from 350 °C to 392 °C for sul-MIL101(Cr) [25]. As to pure-MIL101(Cr), the increasing weight above 400 °C might be related to the transformation from Cr_2O_3 to CrO_x. As to sul-MIL101(Cr), Chromium(III) sulfate might be produced in degradation process, which was stable till 500 °C [31]. Therefore, the weight of sul-MIL-101 remained constant between 400 and 500 °C and then decreased slightly. Both pure-MIL101(Cr) and sul-MIL101(Cr) were thermally stable until 350 °C, which indicated that the MOFs could tolerate the normal operating temperature (<100 °C) for DMFC application.

3.2. Characterization of the hybrid membranes

The morphology of membranes observed by probing cross-sections using FESEM was shown in Fig. 6. It was revealed that

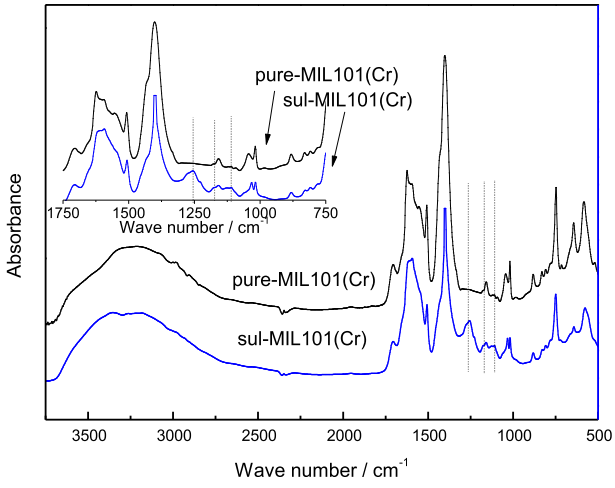

Fig. 3. The IR spectra of pure-MIL101(Cr) and sul-MIL101(Cr).

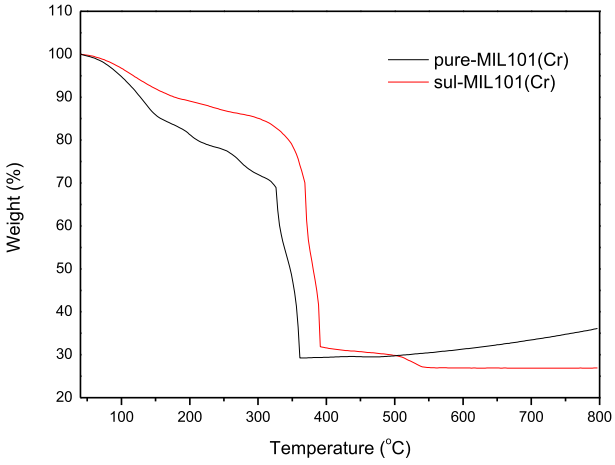

Fig. 5. TGA curve of (a) pure-MIL101(Cr), (b) sul-MIL101(Cr).

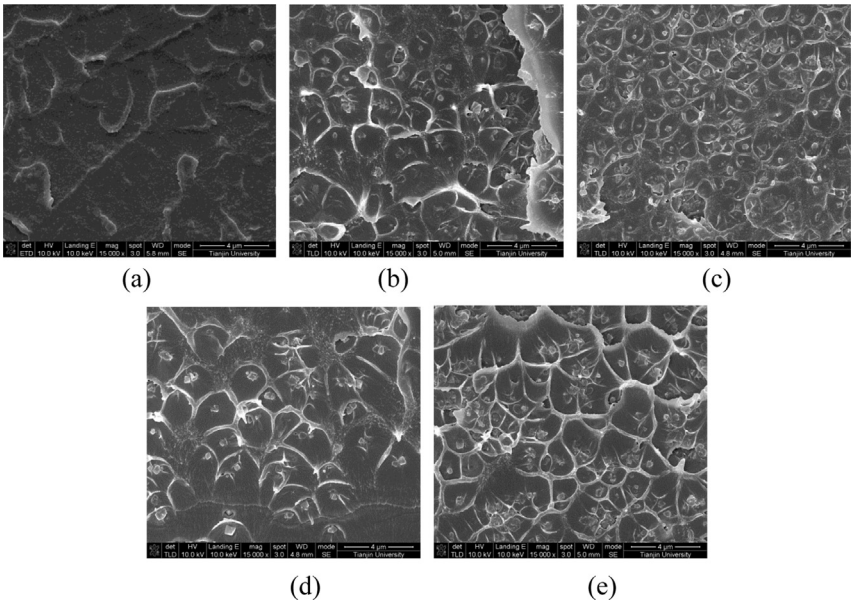

Fig. 6. FESEM images of the cross-section of the pristine membrane and the hybrid membranes: (a) pristine membrane, (b) SPEEK/pure-MIL-5, (c) SPEEK/pure-MIL-7.5, (d) SPEEK/sul-MIL-2.5, (e) SPEEK/sul-MIL-7.5.

hybrid membranes were uniform and defect-free and the MOFs were dispersed homogeneously in hybrid membranes without obvious agglomeration.

TGA was carried out to study the thermal stability of membranes as shown in Fig. 7. It was indicated that all membranes showed similar three-steps weight loss. The first weight loss (below 240 °C) was dedicated by the loss of water and residual solvent in membranes [32,33]. The second weight loss (290 °C–375 °C) was caused by the degradation of sulfonic acid groups. The last weight loss (400 °C–800 °C) was resulted from the degradation of main chains of SPEEK [34]. It could be conjectured that the degradation temperatures of hybrid membranes were almost unchanged and the thermal degradation mechanism of hybrid membranes was unaffected by the incorporated fillers. CrO_x was involatile and could act as a barrier retarding the escape of other volatile substances [27,35]. Therefore, the weight loss of hybrid membranes was lower than that of pristine membrane and the total weight loss decreased with the increasing content of MOFs. It should be noted that the membranes wouldn't be degraded below 290 °C, indicating that the membranes could tolerate the normal operating temperature (<100 °C) for DMFC application.

DSC was performed to determine the glass transition temperatures (T_gs) of the membranes as shown in Fig. 8. T_g of pristine membrane was 155 °C. Incorporation of pure-MIL-101 increased the T_gs of membranes and the T_gs showed continuous increase with increasing filler contents, in part due to the good compatibility between the polymer and the MOFs. By the introduction of pure-MIL-101, both the mobility and flexibility of polymer chains were restrained, which rendered the polymer matrix more compact [36]. On the contrary, the incorporation of sul-MIL-101 decreased T_gs of membranes, and the T_gs was further decreased by increasing filler contents, which was decreased from 155 °C for pristine membrane to 147 °C for SPEEK/sul-MIL-10. It was indicated that both the mobility and flexibility were enhanced by the incorporation of sulfonated MOFs. Sulfonic acid groups on surfaces of MOFs showed electrostatic repulsion with sulfonic acid groups of SPEEK, which disturbed the packing of SPEEK polymer chain and enhanced the motions of local chain [37,38].

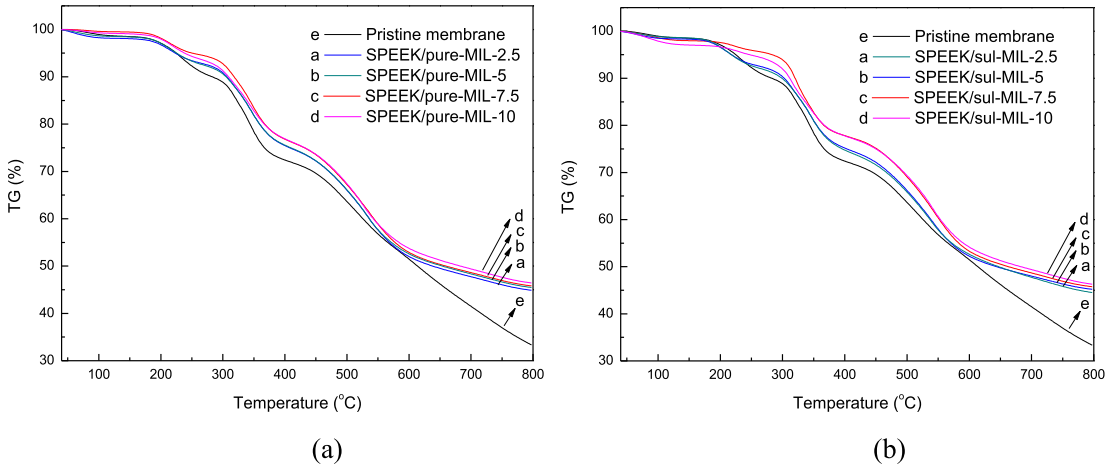

Fig. 7. TGA curves of membranes: (a) pristine membrane and SPEEK/pure-MIL-X and (b) pristine membrane and SPEEK/sul-MIL-X.

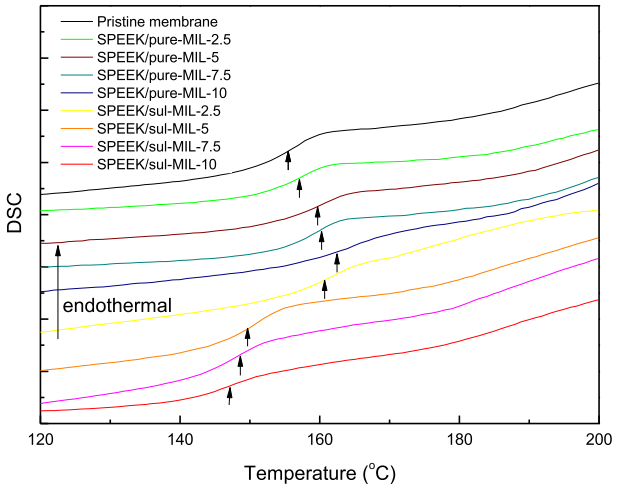

Fig. 8. DSC curve of the pristine membrane, SPEEK/pure-MIL-X and SPEEK/sul-MIL-X.

3.3. Water uptake and area swelling

Water molecules are essential to proton transfer [39,40]. The water uptake and area swelling ratio of membranes were shown in Fig. 9.

Water uptake of pristine membrane was 40.09% and was reduced to 31.6–27.29% and 32.3–30.8% by embedding pure-MIL101(Cr) and sul-MIL101(Cr), respectively. The decrease of water uptake might be caused by the fact that the framework of MIL101 was much more rigid than the SPEEK polymer and was not able to absorb water as much as the polymer matrix by swelling. On the other hand, the hybrid membranes displayed lower area swelling than pristine membrane. Area swelling of pristine membrane was 27.97%, and decreased to 12.74–8.33% for SPEEK/pure-MIL-X and 14.89–11.43% for SPEEK/sul-MIL-X. It might be due to the fact that the interaction between SPEEK and inorganic fillers reduced the free volume of hybrid membranes, leading to the decrease of swelling degree [36].

3.4. Methanol permeability

Methanol permeability of PEMs could greatly influence the performance of fuel cells. The methanol permeability of the membranes was shown in Fig. 10, and the pristine membrane showed a methanol permeability of 6.12×10^{-7} cm^2 s^{-1}. According to the DSC result, the incorporation of pure-MIL-101 restrained both mobility and flexibility of the polymer chains, rendering the polymer matrix more compact, which endowed the SPEEK/pure-MIL-X composite membranes with intensified methanol barrier properties. As a result, the methanol permeability of SPEEK/pure-MIL-X hybrid membranes decreased from 5.80×10^{-7} to 5.14×10^{-7} cm^2 s^{-1} with the filler contents increasing from 2.5 to 10 wt.%. On the contrary, as implied by the DSC result, the incorporation of sul-MIL101 disturbed the packing of SPEEK polymer matrix, enhancing the motions of local chains, which reduced the methanol diffusion resistance. Accordingly, the SPEEK/sul-MIL-X exhibited a higher methanol permeability than SPEEK control membrane. The methanol permeability of SPEEK/sul-MIL-X was increased from 6.15×10^{-7} cm^2 s^{-1} to 7.38×10^{-7} cm^2 s^{-1} by the filler contents from 2.5 to 10 wt.%.

3.5. Proton conductivity

Proton conductivity is a key parameter for a PEM determining fuel cell performance. Proton conductivity of the membranes at different temperatures and 100% RH was measured as shown in Fig. 11. All the membranes exhibited positive temperature-conductivity correlations, indicating a thermally activated process. Pristine membrane with 67.6% DS determined by titration displayed a proton conductivity of 0.054 S cm^{-1} at 30 °C and 100% RH. Incorporation of pure-MIL101(Cr) increased the proton conductivity of SPEEK/pure-MIL101-X, which increased from 0.042 S cm^{-1} to 0.062 S cm^{-1} at 30 °C and 100% RH with the filler contents from 2.5 to 10 wt.% (Fig. 11(a)). In comparison, incorporation of sul-MIL101(Cr) enhanced proton conductivity of the membranes more pronouncedly. SPEEK/sul-MIL-7.5 exhibited the highest proton conductivity of 0.081 S cm^{-1} at 30 °C, which was 49.7% higher than pristine membrane. Proton conductivity of SPEEK/sul-MIL-7.5 was increased to 0.306 S cm^{-1} with increasing temperature to 75 °C, which was 96.2% higher than pristine membrane (0.156 S cm^{-1}).

There were two well accepted mechanisms describing the transfer of proton in PEMs: the vehicle mechanism (the protons diffuse together with water molecules by forming complexes, like 'Zundel' ion and 'Eigen'ion) and Grotthuss mechanism (the protons jump through membranes by continuous breaking and forming of hydrogen bonds) [41,42].

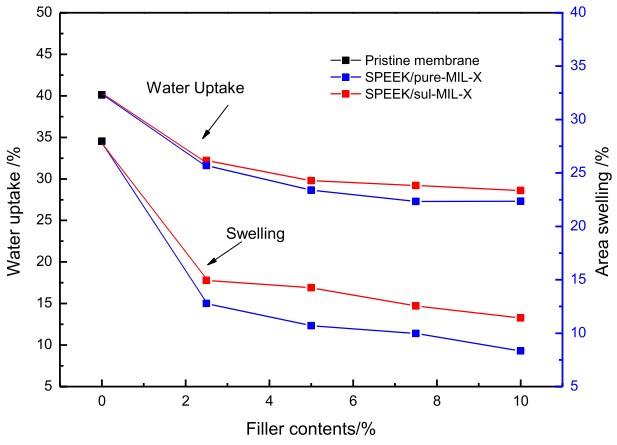

Fig. 9. The water uptake and area swelling properties of the pristine membrane, SPEEK/pure-MIL-X and SPEEK/sul-MIL-X at 25 °C.

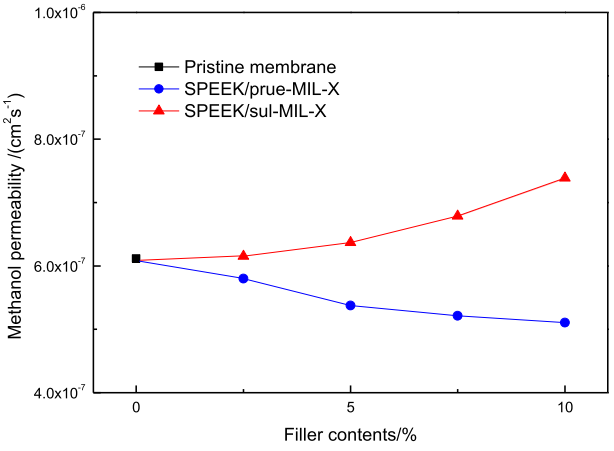

Fig. 10. The methanol permeability of the pristine membrane, SPEEK/pure-MIL-X and SPEEK/sul-MIL-X at 25 °C.

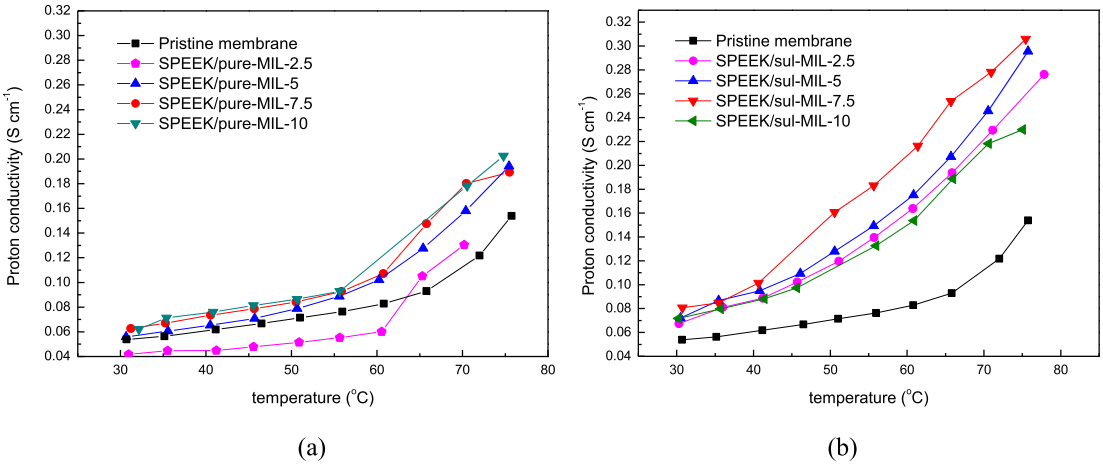

Fig. 11. Proton conductivity of the pristine membrane and hybrid membranes as a function of temperature at 100% RH: (a) SPEEK/pure-MIL101(Cr), (b) SPEEK/sul-MIL101(Cr).

Incorporation of pure-MIL might have two opposite impacts on the proton conductivity of membrane. On one hand, SPEEK matrix became more compact than pristine membranes after the incorporation of the pure-MIL101(Cr), leading to decreased proton conductivity. On the other hand, MIL101(Cr) was rich in coordinatively unsaturated metal sites (CUSs), which belonged to Lewis acid and could provide a large amount of −OH by hydrolysis. These −OH groups could form hydrogen-bonded networks, leading to elevated proton conduction by Grotthuss mechanism [5,10,11,20]. At low filler content (2.5 wt.%), the amount of CUSs and bound water was too little to construct effective hydrogen-bonded networks. Thus, the former factor was dominant, resulting in decreased proton conductivity. The hydrolysis could be enhanced along with increasing temperature, and the amount of CUSs could increase along with the increased filler contents, which resulted in that the latter factor began to hold dominant position, leading to increased proton conductivity.

The proton conductivity of the membrane was enhanced significantly by incorporating sul-MIL101(Cr) compared with those of the pristine SPEEK membrane and SPEEK/pure-MIL101 membranes, mainly due to the following two aspects: i) extra sulfonic acid groups grafted in the MOFs rendered more facile hopping sites for proton conduction [9,43–45]; ii) sulfonic acid groups coupled with water molecules at the SPEEK/MOFs interfaces might form additional pathway for proton conduction [45,46].

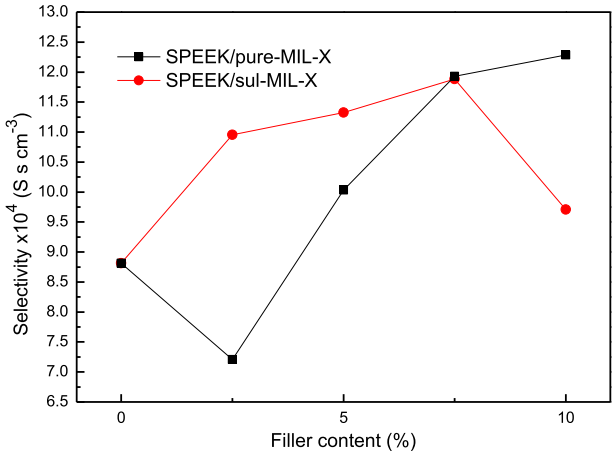

Fig. 12. Selectivity of the pristine membrane and hybrid membranes at 30 °C.

3.6. Selectivity of membranes

Selectivity which is defined as the ratio of proton conductivity to methanol permeability is often employed to evaluate the potential performance of a DMFC membrane. As shown in Fig. 12, the selectivity of pristine SPEEK membrane was 8.8×10^4 S s cm^{-3}. The selectivity of SPEEK/pure-MIL-X hybrid membranes was lower than pristine SPEEK membrane at the filler content of 2.5 wt.% because of the low proton conductivity, and then increased with the increased filler contents. The highest selectivity was 12.3×10^4 S s cm^{-3} at the filler content of 10 wt. %,. As for SPEEK/sul-MIL-X, the selectivity increased from 11.0×10^4 S s cm^{-3} to 11.9×10^4 with the filler contents in the range of 2.5–7.5 wt.%, and then the selectivity began to decrease because of the increased methanol permeability and decreased proton conductivity. The selectivity of SPEEK/sul-MIL-X was higher than that of both SPEEK/pure-MIL-X and pristine membrane owing to their high proton conductivity at the filler contents of 2.5–7.5 wt. %.

4. Conclusion

In this study, a novel kind of hybrid membrane was prepared by incorporating sul-MIL101(Cr) into SPEEK. Although the methanol permeability was increased slightly, the proton conductivity of hybrid membranes was increased significantly. The increased proton conductivity could be attributed to the sulfonated MOFs with multiple functionalities in hybrid membranes: i) providing sulfonic acid groups as facile proton hopping sites; ii) forming additional proton-transport pathway at the interfaces of polymer and MOFs; iii) constructing hydrogen-bonded networks for proton conduction via the hydrolysis of CUSs. By incorporation of sul-MIL101(Cr), the hybrid membranes exhibited a high proton conductivity of 0.306 S cm^{-1} at 75 °C, 100% RH, which is 96.2% higher than that of pristine membranes. It was inspired that acid functionalized MOFs had great application potential in proton conductive membranes, and our study may contribute a new idea for fabricating high proton conducting hybrid membranes.

Acknowledgments

We gratefully acknowledge financial support from National Science Fund for Distinguished Young Scholars (21125627), the National High Technology Research and Development Program of

China (2012AA03A611), and the Program of Introducing Talents of Discipline to Universities (No. B06006).

References

[1] B. Panella, M. Hirscher, Adv. Mater. 17 (2005) 538–541.
[2] H. Wu, J.M. Simmons, Y. Liu, C.M. Brown, X.S. Wang, S.Q. Ma, V.K. Peterson, P.D. Southon, C.J. Kepert, H.C. Zhou, T. Yildirim, W. Zhou, Chem. Eur. J. 16 (2010) 5205–5214.
[3] V. Stavila, R.K. Bhakta, T.M. Alam, E.H. Majzoub, M.D. Allendorf, Acs Nano 6 (2012) 9807–9817.
[4] S. Ye, X. Jiang, L.W. Ruan, B. Liu, Y.M. Wanga, J.F. Zhu, L.G. Qiu, Microporous Mesoporous Mater. 179 (2013) 191–197.
[5] C. Wang, D. Liu, W. Lin, J. Am. Chem. Soc. 135 (2013) 13222–13234.
[6] D. Jiang, T. Mallat, F. Krumeich, A. Baiker, J. Catal. 257 (2008) 390–395.
[7] F.X.L. Xamena, O. Casanova, R.G. Tailleur, H. Garcia, A. Corma, J. Catal. 255 (2008) 220–227.
[8] G.K.H. Shimizu, J.M. Taylor, S.R. Kim, Science 341 (2013) 354–355.
[9] T. Yamada, M. Sadakiyo, H. Kitagawa, J. Am. Chem. Soc. 131 (2009) 3144–3145.
[10] S. Ohkoshi, K. Nakagawa, K. Tomono, K. Imoto, Y. Tsunobuchi, H. Tokoro, J. Am. Chem. Soc. 132 (2010) 6620–6621.
[11] N.C. Jeong, B. Samanta, C.Y. Lee, O.K. Farha, J.T. Hupp, J. Am. Chem. Soc. 134 (2012) 51–54.
[12] M. Sadakiyo, H. Okawa, A. Shigematsu, M. Ohba, T. Yamada, H. Kitagawa, J. Am. Chem. Soc. 134 (2012) 5472–5475.
[13] J.A. Hurd, R. Vaidhyanathan, V. Thangadurai, C.I. Ratcliffe, I.L. Moudrakovski, G.K.H. Shimizu, Nat. Chem. 1 (2009) 705–710.
[14] J.M. Taylor, R.K. Mah, I.L. Moudrakovski, C.I. Ratcliffe, R. Vaidhyanathan, G.K.H. Shimizu, J. Am. Chem. Soc. 132 (2010) 14055–14057.
[15] J.M. Taylor, K.W. Dawson, G.K.H. Shimizu, J. Am. Chem. Soc. 135 (2013) 1193–1196.
[16] J.M. Taylor, R. Vaidhyanathan, S.S. Iremonger, G.K.H. Shimizu, J. Am. Chem. Soc. 134 (2012) 14338–14340.
[17] V.G. Ponomareva, K.A. Kovalenko, A.P. Chupakhin, D.N. Dybtsev, E.S. Shutova, V.P. Fedin, J. Am. Chem. Soc. 134 (2012) 15640–15643.
[18] M. Sadakiyo, T. Yamada, H. Kitagawa, J. Am. Chem. Soc. 131 (2009) 9906–9907.
[19] X.Q. Liang, F. Zhang, W. Feng, X. Zou, C.J. Zhao, H. Na, C. Liu, F.X. Suna, G.S. Zhu, Chem. Sci. 4 (2013) 983–992.
[20] B. Wu, X.C. Lin, L. Ge, L. Wua, T.W. Xu, Chem. Commun. 49 (2013) 143–145.
[21] A. Shigematsu, T. Yamada, H. Kitagawa, J. Am. Chem. Soc. 133 (2011) 2034–2036.
[22] M. Yoon, K. Suh, S. Natarajan, K. Kim, Angew. Chem. Int. Ed. 52 (2013) 2688–2700.
[23] S.J. Paddison, K.D. Kreuer, J. Maier, Phys. Chem. Chem. Phys. 8 (2006) 4530–4542.
[24] A. Iulianelli, A. Basile, Int. J. Hydrogen Energy 37 (2012) 15241–15255.
[25] G. Ferey, C. Mellot-Draznieks, C. Serre, F. Millange, J. Dutour, S. Surble, I. Margiolaki, Science 309 (2005) 2040–2042.
[26] M.G. Goesten, J. Juan-Alcañiz, E.V. Ramos-Fernandez, K.B.S.S. Gupta, E. Stavitski, H.V. Bekkum, J. Gascon, F. Kapteijn, J. Catal. 281 (2011) 177–187.
[27] Y.N. Zhao, Z.Y. Jiang, D.S. Lin, A.J. Dong, Z. Li, H. Wu, J. Power Sources 224 (2013) 28–36.
[28] A. Khutia, H.U. Rammelberg, T. Schmidt, S. Henninger, C. Janiak, Chem. Mater. 25 (2013) 790–798.
[29] S.R. Kelemen, G.N. George, M.L. Gorbaty, Fuel 69 (1990) 939–944.
[30] Q.H. Yang, J. Liu, J. Yanga, M.P. Kapoor, S.J. Inagaki, C. Li, J. Catal. 228 (2004) 265–272.
[31] K.T. Jacob, D.B. Rao, H.G. Nelson, Metall. Mater. Trans. A 10 (1979) 327–331.
[32] L.L. Nie, J.T. Wang, T. Xu, H. Dong, H. Wu, Z.Y. Jiang, J. Power Sources 213 (2012) 1–9.
[33] M.N.A.M. Norddin, A.F. Ismail, D. Rana, T. Matsuura, S. Tabe, J. Membr. Sci. 328 (2009) 148–155.
[34] P.X. Xing, G.P. Robertson, M.D. Guiver, S.D. Mikhailenko, K.P. Wang, S. Kaliaguine, J. Membr. Sci. 229 (2004) 95–106.
[35] H. Zou, S.S. Wu, J. Shen, Chem. Rev. 108 (2008) 3893–3957.
[36] G.W. He, Y.F. Li, Z.Y. Li, L.L. Ni, H. Wu, X.L. Yang, Y.N. Zhao, Z.Y. Jiang, J. Power Sources 248 (2014) 951–961.
[37] A.G. Kannan, N.R. Choudhury, N.K. Dutta, J. Membr. Sci. 333 (2009) 50–58.
[38] J.T. Wang, X.J. Yue, Z.Z. Zhang, Z. Yang, Y.F. Li, H. Zhang, X.L. Yang, H. Wu, Z.Y. Jiang, Adv. Funct. Mater. 22 (2012) 4539–4546.
[39] B.J.P. Tripathi, V.K. Shahi, Prog. Polym. Sci. 36 (2011) 945–979.
[40] J. Ren, S.L. Zhang, Y. Liu, Y. Wang, J.H. Pang, Q.H. Wang, G.B. Wang, J. Membr. Sci. 434 (2013) 161–170.
[41] N.B. Hara, H. Ohashi, T. Ito, T. Yamaguchi, J. Phys. Chem. B 113 (2009) 4656–4663.
[42] K.D. Kreuer, Chem. Mater. 8 (1996) 610–641.
[43] W.J. Phang, W.R. Lee, K. Yoo, B. Kim, C.S. Hong, Dalt. Trans. 42 (2013) 7850–7853.
[44] R. Kannan, B.A. Kakade, V.K. Pillai, Angew. Chem. Int. Ed. 47 (2008) 2653–2656.
[45] T. Xu, W.Q. Hou, X.H. Shen, H. Wu, X.C. Li, J.T. Wang, Z.Y. Jiang, J. Power Sources 196 (2011) 4934–4942.
[46] Y.F. Li, G.W. He, S.F. Wang, S.N. Yu, F.S. Pan, H. Wu, Z.Y. Jiang, J. Mater. Chem. 1 (2013) 10058–10077.